Replication of alphaviruses requires a pseudoknot that involves the poly(A) tail

RENÉ C.L. OLSTHOORN

Leiden Institute of Chemistry, Leiden University, 2300 RA Leiden, The Netherlands

ABSTRACT

Alphaviruses, such as the Sindbis virus and the Chikungunya virus, are RNA viruses with a positive sense single-stranded RNA genome that infect various vertebrates, including humans. A conserved sequence element (CSE) of ~19 nt in the 3′ noncoding region is important for replication. Despite extensive mutational analysis of the CSE, no comprehensive model of this element exists to date. Here, it is shown that the CSE can form an RNA pseudoknot with part of the poly(A) tail and is similar to the human telomerase pseudoknot with which it shares 17 nt. Mutants that alter the stability of the pseudoknot were investigated in the context of a replicon of the Sindbis virus and by native gel electrophoresis. These studies reveal that the pseudoknot is required for virus replication and is stabilized by UAU base triples. The new model is discussed in relation to previous data on Sindbis virus mutants and revertants lacking (part of) the CSE.

Keywords: alphavirus; base triple; poly(A) tail; pseudoknot

INTRODUCTION

For RNA viruses it is known that the secondary and tertiary structure of their RNA genome plays an important role in many aspects of their life cycle. RNA viruses have evolved a large variety of RNA structures that are required for replication of their genome (Ahlquist 1992; You and Rice 2008; Liu et al 2009, 2020; Pflug et al. 2014), regulating their translation (Brierley et al. 1989; Miras et al. 2017; Jaafar and Kieft 2019; Bhatt et al. 2021), packaging progeny RNA (Carey et al. 1983; Turner et al. 1988; Frolova et al. 1997; Masters 2019; Ding et al. 2020), or derailing host defense mechanisms (Pijlman et al. 2008; Akiyama et al. 2016; Flobinus et al. 2016; Dilweg et al. 2019). In many instances, the 3′-end of plus strand RNA viruses was found to fold into a pseudoknot structure that plays an essential role in the synthesis of a minus-strand copy of the genomic RNA (Rietveld et al. 1983; Pilipenko et al. 1992; Kolk et al. 1998; Tsai et al. 1999; Pogany et al. 2003), sometimes in direct equilibrium with an alternate conformation consisting of stem–loop structures that performs a different function in the viral life cycle (Olsthoorn et al. 1999; Dreher 2009).

Alphaviruses are RNA viruses with a positive-sense single-stranded RNA genome that are found nearly worldwide and include Sindbis virus (SINV), Chikungunya virus (CHIKV), and Eastern and Western equine encephalitis viruses. They are transmitted by mosquitos and infect various vertebrates such as humans, horses, rodents, fish, and birds as well as invertebrates, causing mostly arthritis and encephalitis. SINV infection of humans mostly occurs in Northern Europe where it is endemic (https://www.ecdc.europa.eu/en/sindbis-fever/facts). CHIKV is endemic in tropical Africa and Asia, though outbreaks have occurred in Italy (Charrel et al. 2007), India (Ramachandran et al. 2012), and more recently in Central America and the Caribbean (Morrison 2014). Since then, CHIKV has been isolated on many continents including North and South America, Europe, and Australia (Levi and Vignuzzi 2019). Presently, no antivirals or vaccines against alphaviruses are commercially available.

The genome of alphaviruses is 11–12 kilobases in length and possesses a 5′ cap structure and a 3′ poly(A) tail. The 5′ two-thirds of the genome encode the polymerase proteins. The capsid protein is encoded by a subgenomic mRNA (26S RNA). Among the studied cis-acting signals are elements needed for 26S RNA synthesis (Levis et al. 1990), encapsidation (Kim et al. 2011), and replication (Hyde et al. 2015; Kendall et al. 2019). Two important elements required for production of minus-strand RNA have previously been identified: an RNA structure in the

5′ untranslated region (UTR) (Niesters and Strauss 1990; Frolov et al. 2001) and a conserved sequence element (CSE) in the 3′-UTR of ~19 nt (Levis et al. 1986). The 5′-UTR hairpin has been shown to bind to the viral RNA-dependent RNA polymerase (RdRp) (Frolov et al. 2001). The role of the CSE in minus-strand synthesis has been investigated in vivo (Kuhn et al. 1990; Raju et al. 1999) and in vitro (Hardy and Rice 2005; Hardy 2006). Whereas single substitutions in the CSE can be lethal to the virus, several large deletions in the CSE are tolerated and even complete removal of the CSE can result in viable virus (Kuhn et al. 1990; Raju et al. 1999). In vitro assays have indicated that a poly(A) tail of at least 11–12 residues is required to get some minus-strand synthesis, but that 25 A's allow maximal synthesis (Hardy and Rice 2005). Single substitutions in the CSE are in general detrimental for RNA synthesis, although insertions are often tolerated. Altogether, the mutational analyses have not led to a comprehensive model for the structure of the CSE in alphaviruses.

Here the possibility of pseudoknot formation by the CSE and part of the poly(A) tail in alphaviruses is investigated. Using Sindbis virus replicons harboring GFP or luciferase reporter genes, it is demonstrated that this pseudoknot structure is essential for viral replication. In addition, native gel electrophoresis shows that the pseudoknot is stabilized by UAU base triples by analogy to the telomerase RNA pseudoknot. The new model is discussed in relation to previous data on viable SINV mutants and revertants lacking (part of) the CSE.

RESULTS

Conserved sequence element (CSE) can fold into a pseudoknot

The CSE has been found to be strongly conserved among alphaviruses (Pfeffer et al. 1998); however, the significant variation in its length, 16–21 nt, suggests that the CSE may not function as a linear sequence. By including the poly(A) tail in the alignment, it becomes clear that Watson–Crick base pairs can be formed between nucleotides at the 5′ end of CSE and its 3′-end, plus several A's from the poly(A) tail (highlighted in green in Fig. 1A). This interaction is supported by covariations: the G_{-14}–C_{-1} base pair (bp) in SINV is a UA bp in Sagiyama (SAG), Getah (GET), Ross River (RR), Barmah Forest (BF) viruses and in two Eastern equine encephalitis virus (EEEV) isolates. Vice versa, the U_{-15}–A_{+1} bp in SINV is a GC bp in SAG, GET, RR, BF, Middelburg (MIDV), Bebaru, Una, and in fish alphaviruses. Likewise, the U_{-18}–A_{+4} bp is replaced by an AU bp in several fish alphaviruses. The resulting hairpin is illustrated for several alphaviruses in Figure 1B. The loop of 10–14 nt includes two stretches of U residues that can form a pseudoknot with the poly(A) tail, as shown in Figure 1C.
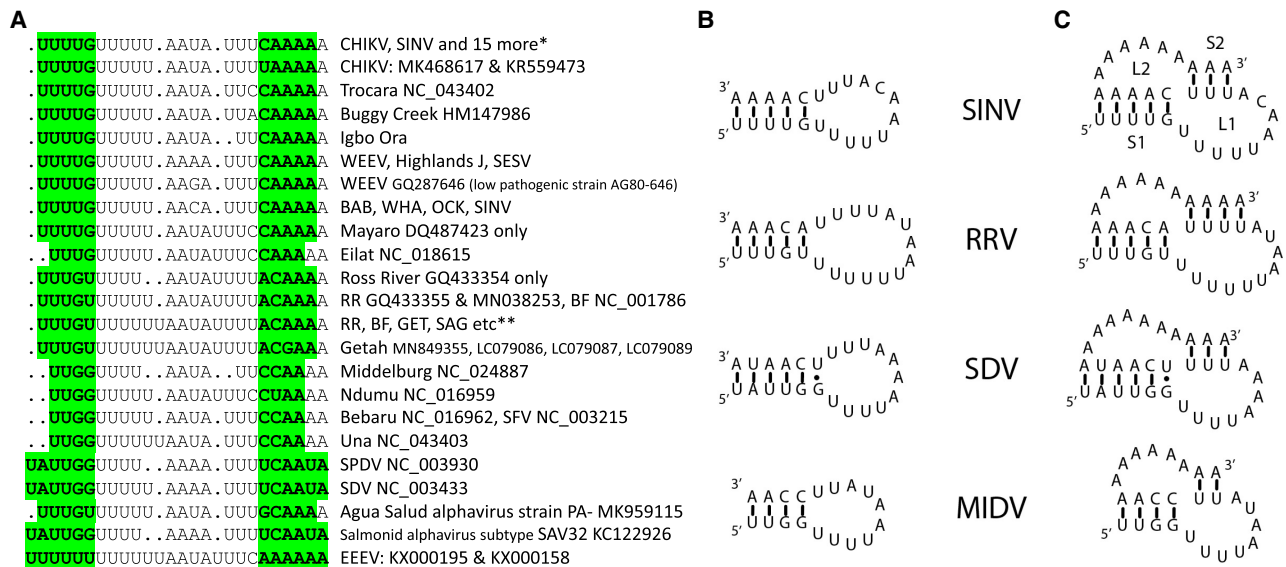
FIGURE 1. (*A*) Alignment of CSE from all known alphaviruses to date for which the 3′-end is complete. (*) CHIKV NC_004162, Mayaro NC_003417, VEEV Venezuelan Equine Encephalitis virus NC_001449, Aura NC_003900, EEEV Eastern Equine Encephalitis virus NC_003899, Madariaga NC_023812, Mucambo NC_038672, Mwinilunga LC361437, Tai Forest NC_032681, Fort Morgan NC_013528, Cabassou NC_038670, Rio Negro NC_038674, Mosso das Pedras NC_038857, Pixuna NC_038673, Tonate NC_038675, Everglades NC_038671, O'nyong nyong NC_001512, Igbo Ora AF079457, SINV NC_001547, WEEV Western equine encephalitis virus NC_003908, Highlands J NC_012561, SESV Southern elephant seal virus HM147990, Babanki HM147984, Whataroa NC_016961, Ockelbo M69205, SINV MF589985, MF409177. (****)** Ross River MH987781 plus others, Barmah Forest MN115377 plus others, Alphavirus M1 EF011023, Getah NC_006558, Sagiyama AB032553. (*B*) Putative hairpin structures formed by the CSE in diverse alphaviruses. (SDV) Sleeping disease virus. (*C*) Putative pseudoknot structures involving the poly(A) tail.

The number of A residues that is required to allow pseudoknot formation in SINV is estimated to be ~12: four A's in stem S1 and three A's in stem S2, plus another five to six A's in L2, the loop that crosses the minor groove of S1 (Fig. 1C). The minor groove of a 5-bp stem is ~25 Ångstroms (Pleij et al. 1985), which would require at least five A's to span the minor groove. Six A's are chosen here as one adenosine is predicted to pair with a uracil in L1 (see below). The number of 12 A's fits well with the experimentally determined minimum number of 11–12 A's that are required for minus-strand synthesis in vitro using SINV RNA (Hardy and Rice 2005).

Minimum length of poly(A) tail required for replication

To determine the minimal length of the poly(A) tail required for in vivo replication, mutations were introduced via PCR using a SINV replicon expressing GFP (Bredenbeek et al. 1993). In vitro transcribed and capped mRNAs were transfected into BHK21 cells, and the number of GFP positive cells was counted ~20 h post-transfection. A construct carrying a 29-nt poly(A) tail (SinA29 or SinA for short) served as a wild-type control against which all further constructs were tested. Shortening the length of the poly(A) tail to 20 A's had a minor effect on the number of GFP-positive cells, but at 14, 11, and eight A's an approximately threefold reduction in the number of GFP-positive cells was observed (Fig. 2). This reduction was even more dramatic with four A's (~1%), and without a poly(A) tail virtually no GFP-positive cells were visible. This suggests that below eight A's, a critical length is reached that severely impairs replication of the virus.

To investigate to what extent the length of the poly(A) tail affects the translation of SINV RNA, transfections with a *Renilla* luciferase mRNA harboring the 3′-UTR of SINV with different lengths of the poly(A) tail were performed. Shortening the poly(A) tail from 29 to 20 residues appeared

to increase translation, while further truncation to 14 and 11 A's reduced translation to 78% and 65%, respectively (Fig. 2B). Interestingly, the constructs with four or zero A's still supported a substantial level of translation (54%–67%). This suggests that the low or absent replication of SINV RNAs with four or less A's is predominantly due to a defect in RNA synthesis by the inability to form the pseudoknot, rather than in translation.

Base-pairing in stem 1 contributes to replication

To investigate whether the individual stems of the proposed pseudoknot are required for replication, base pairs were disrupted and restored by secondary mutations. Although in these assays the relative replication levels of mutants with respect to wt were calculated by comparing the number of GFP-positive cells, these levels were treated in a semiquantitative manner based on the indicated five categories (Fig. 3, inset). As G_{-14} and C_{-1} are strongly conserved nucleotides in the CSE and contribute to the formation of stem S1, they were subjected to mutational analysis first. Disruption of the G_{-14}–C_{-1} bp led to a significant decrease in replication (Fig. 3, SinB1), whereas restoring base-pairing by the introduction of an AU bp increased replication with respect to the AC mismatch (Fig. 3, SinB2). The AU bp was still worse than wt, but this may be due to its lower thermodynamic stability. Disruption of the U_{-15}–A_{+1} bp also reduced replication, but this could be restored to wt level by a GC bp (Fig. 3, SinC1 and SinC2). Likewise, disruption of two UA bps in S1, thereby essentially disrupting stem 1, resulted in a low level of replication, but restoring stem 1 by formation of AU bps resulted in a significant increase in replication (Fig. 3, SinD1 and SinD2). Finally, replacing S1 with GC-richer stems did reduce replication (Fig. 3, SinE2, SinF, SinG), but also here mismatches reduced replication even more (Fig. 3, SinE1).

From these results it can be concluded that nucleotides U_{-18} to G_{-14} of the SINV CSE do not function as a linear
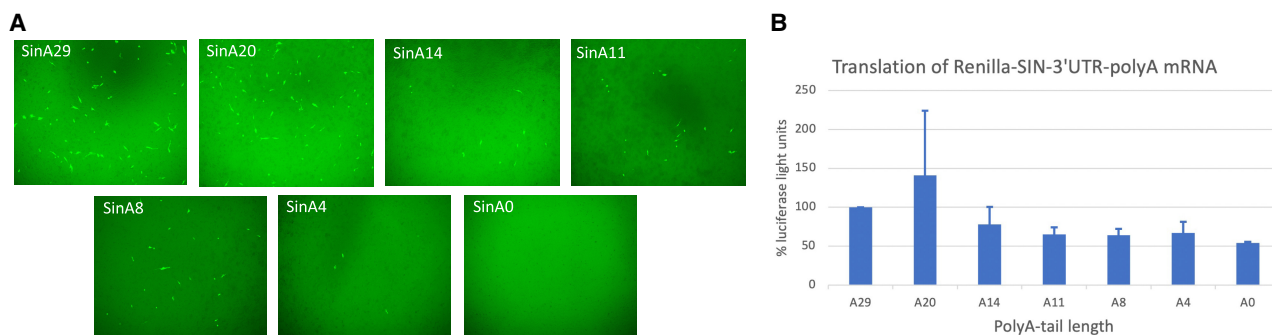
FIGURE 2. Effect of poly(A) tail length on replication and translation. (*A*) GFP expression in BHK21J cells transfected with SINV replicon RNAs harboring different sizes of the poly(A) tail. Images show a representative area of a 48-well plate and are intentionally overexposed to show the density of cells present in this area of the plate. (*B*) Luciferase expression in BHK21J cells transfected with *Renilla* luciferase mRNAs harboring the 3′-UTR of SINV with the indicated length of the poly(A) tail. Error bars indicate standard deviation of two independent experiments.
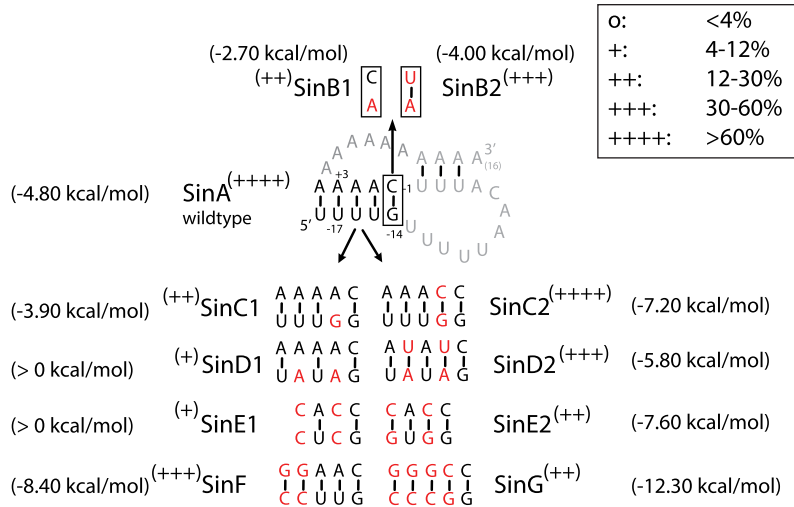
FIGURE 3. Role of S1 length and stability for replication. The minimum free energy for each S1 was calculated using Mfold (Zuker 2003). Percentages were calculated from at least two independent transfections using wild-type SinA as 100% control.

sequence but are base-paired to C_{-1} and four A's of the poly(A) tail, thereby forming a stem whose thermodynamic stability can only be varied within certain limits and/or whose nucleotide composition may be restricted by the requirement for tertiary contacts.

## Base pairs in stem 2 are involved in base triples

Stem 2 is predicted to consist of two (e.g., MIDV), three (e.g., CHIKV, SINV, SDV), or four bps (e.g., RRV) in the different alphaviruses (Fig. 1A). Insertion of an additional U residue in SINV PK, thereby creating a 4-bp stem 2, had no significant effect on replication (Fig. 4, SinH). Deletion of one U resulting in a 2-bp stem 2, on the other hand, significantly decreased replicon activity (Fig. 4, SinI). In the context of the MIDV CSE, two UA bps in S2 were less detrimental for replication (Fig. 4, inset). This is probably due to the higher stability of S1, as the C to U change in loop L1 has no significant effect on replication (Supplemental Fig. S2; Kuhn et al. 1990; Hardy and Rice 2005). Disruption of the $U_{-2}A_{+11}$ bp (SinJ) or the $U_{-3}A_{+12}$ bp (SinK1), thereby creating a CA mismatch in stem 2, resulted in a reduced or slightly reduced level of replication (Fig. 4). Repairing the CA mismatch in SinK1 by creating a CG match did not increase activity but decreased activity even more (Fig. 4, SinK2). Although this result would suggest that nucleotides at positions −3 and +12 are not forming a base pair, it is also possible that the UA bps in stem 2 are involved in base triples with U residues in L1, as has been shown, for example, for the telomerase pseudoknot, Kaposi's sarcoma-associated herpesvirus (KSHV), polyadenylated nuclear RNA and MALAT-1 noncoding RNA (Theimer et al. 2005; Mitton-Fry et al. 2010; Brown et al. 2012). In those

studies, UAU base triples could be replaced with isosteric CGC triples. Such a strategy would also tell which U residues are involved in which base triples in SINV, because beforehand it is difficult to predict whether SINV adopts the KSHV or the telomerase-like PK (Fig. 5).

To find out whether the SINV pseudoknot adopted the KSHV-like structure, mutations were made in a putative base triple between U_{-3}, A_{+13}, and U_{-12} (Fig. 5B). As illustrated by the number of GFP-positive cells, replication of SinM was a lot worse than wt (SinA). However, replication of SinN, which possessed a putative CGC triple, was even worse (Fig. 5B). This could mean that the SINV PK does not form base triples at all or that it adopts a telomerase-like PK with base triples in another register. To investigate the latter possibility, the putative triple formed by $U_{-3}A_{+12}U_{-11}$ was disrupted by changing the U's to C's. This basically abolished replication (Fig. 6A, SinO). However, restoring the base triple with the isosteric CGC triple effectively restored replication (Fig. 6A, SinP). This strongly suggested that the SINV PK favors a telomerase-like PK conformation. Although CGC triples require protonation of one of the cytosines, which in vitro can be achieved by lowering the pH, CGC triples are naturally present in a variety of RNAs (Devi et al. 2015), suggesting that in vivo protonation does occur.

To investigate whether the other two UA pairs are also stabilized by a base triple, they were replaced by CGC
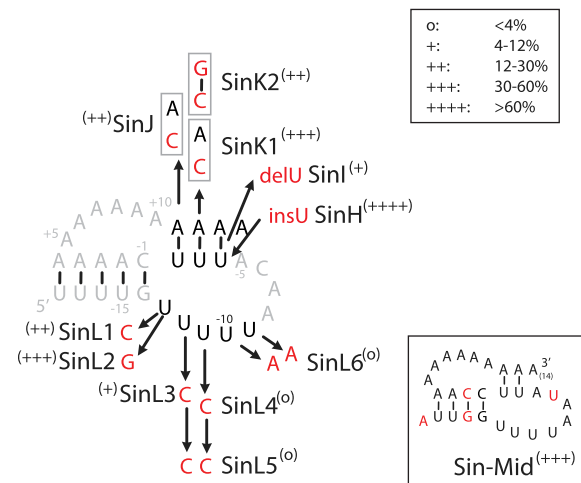
FIGURE 4. Stem 2 and Loop 1 mutants. Percentages were calculated from at least two independent transfections using wild-type SinA as 100% control.
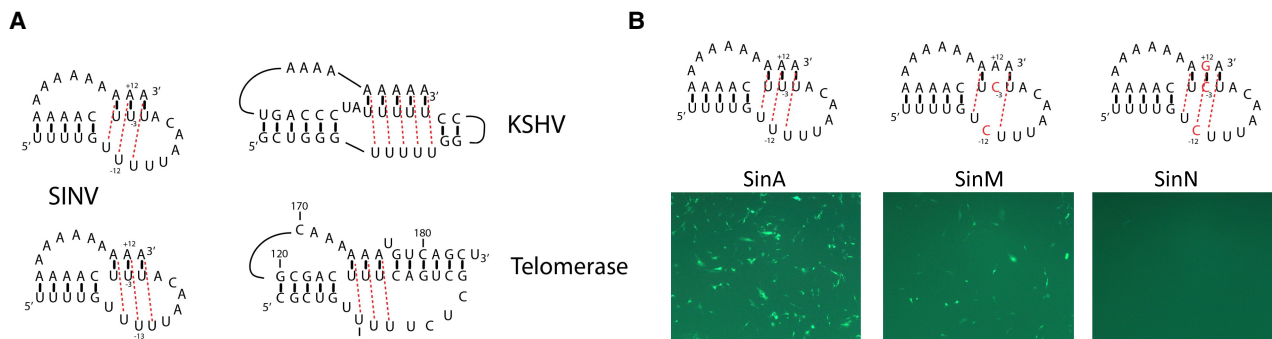
FIGURE 5. (A) Putative base triples in the SINV pseudoknot, adopting either a KSHV-like conformation (*top*) or a human telomerase pseudoknot-like conformation (*bottom*). Red dotted lines indicate Hoogsteen base-pairing of U with an AU base pair. (B) Testing the KSHV-like pseudoknot conformation by mutating a putative base triple between U_{-3}, A_{+13}, and U_{-12} using the SINV replicon.

triples as well. As can be seen in Figure 6, mutation of U_{-2} and U_{-12} (SinQ) or U_{-4} and U_{-10} (SinS) abolished replication, whereas introduction of CGC triples (SinR and SinT) was able to restore replication significantly, although not to wt levels. These results were largely confirmed by using SINV replicons in which the GPF gene was replaced by a nanoluciferase gene (Fig. 6B).

Additional mutations of the middle UAU triple confirmed that UAU or CGC combinations are fully functional at this position in the pseudoknot. Mutation of U_{-11} to C was by itself sufficient to virtually knock out replication completely (Fig. 4, SinL4), and a UGC combination was also quite detrimental (Fig. 6, SinU). Interestingly, replacing A_{+12} by a G had hardly any effect (Fig. 6, SinV). Although the resulting UGU triple could partially, between 5 and 30%, depending on its location, substitute for a UAU triple in MALAT-1 RNA (Brown et al. 2012), it is more likely that in this case the change is accommodated in the structure by a shift in register of the poly(A) tail, thereby decreasing or enlarging the size of the A-rich loop.

The importance of U_{-10} U_{-11} U_{-12} residues was further emphasized by mutants $U_{-12}C$ (Fig. 4, SinL3), $U_{-12}C+U_{-11}C$ (SinL5) and $U_{-10}A+U_{-9}A$ (SinL6), which all resulted in zero or close to zero replication (Fig. 4). U_{-13} on the other hand is, by analogy with U_{99} in the telomerase pseudoknot (Fig. 5), probably involved in a Hoogsteen base pair with A_{+10}. Replacing U_{-13} by a C (Fig. 4, SinL1) reduced replication more than replacing U_{-13} by a G (SinL2), which in principle can form a similar Hoogsteen pair with A_{+10}. These results provide additional support for a telomerase pseudoknot-like structure of the SINV 3'-end.

## Native gel-electrophoresis

To gain more insight into structural effects caused by mutations in the SINV pseudoknot, native gel-electrophoresis with short RNA oligonucleotides was performed. Three SINV-like RNAs, SINA, SINB and SINC of 33 nt, were stud-

ied. These constructs carried two GC base-pair substitutions at the 5′ proximal end of S1 to stabilize the pseudoknot, as initially the wt sequence of the SINV pseudoknot, adopted too many conformations to be useful for native PAGE (data not shown). SINA resembles the pseudoknot of the SinF construct which was replicating close to wt level (Fig. 3). As can be seen in Figure 7, SINA migrated faster than SINB, which is indicative of a more compact structure. Introduction of a CGC triple (SINC), however, did not result in a wt-like migration; in fact its migration was even less than that of SINB. As the C in CGC triples needs to be protonated to form two hydrogen bonds with guanine, and the running buffer and gel had a pH of 8.3, the samples were rerun under acidic conditions. Interestingly, at pH 5.5, SINC now migrated faster than SINB and as fast as SINA, indicating that protonation indeed promotes formation of the CGC triple.

Similar results were obtained with the shorter MIDV pseudoknot (27 nt). Figure 8 shows that at pH 8.3, MidA migrated faster than mutants that had double (MidB) U to C changes and also faster than MidC with the CGC triple. Again, at pH5.5 MidC caught up with MidA while MidB did not, indicating that in MidC the CGC triple is stabilized under acidic conditions.

DISCUSSION

The data presented in this work strongly suggest that the SINV CSE is not functioning as a linear sequence but as a pseudoknot involving part of the poly(A) tail. The presence of a similar pseudoknot in all alphavirus RNAs is supported by covariations in the base-pair composition of stem 1. As stem 2 of the pseudoknot consists solely of base pairs that involve the poly(A) tail, no covariations are found here; the existence of stem 2 in SINV was proven here by replacing the three predicted UAU base triples with CGC triples. In the majority of other alphaviruses, three UAU triples are also predicted although some viruses can form four (Fig.
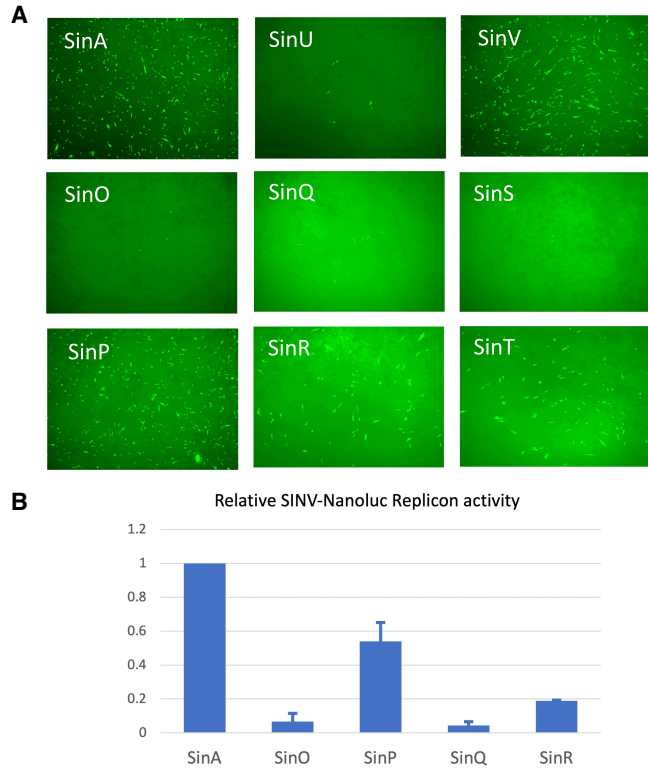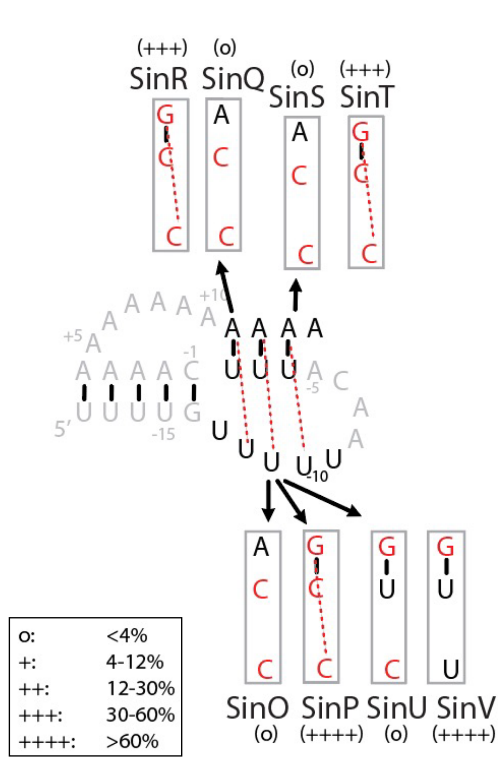
FIGURE 6. Disruption and restoration of base triples in SINV pseudoknot. (*A*) GFP expression in BHK21J cells transfected with SINV replicons carrying the indicated changes in the pseudoknot. (*B*) Relative nanoluciferase expression of BHK21J cells transfected with SINV-Nanoluc replicons. Error bars indicate standard deviation of two experiments.

1, e.g., Ross River, Barmah Forest, Getah, and Sagiyama viruses). Four viruses, MIDV, Trocara, Buggy Creek, and Igbo Ora virus, can only form two triples (Fig. 1A), but as shown here for MIDV using native gel-electrophoresis, this still allows pseudoknot formation.

As the pseudoknot structure depends on the poly(A) tail, a certain number of A's must be present to allow its formation. It was found here that a minimum number of eight A residues is sufficient to sustain a substantial level of replication compared to SINV RNA that has 29 A's. Eight A residues are in principle sufficient to form a pseudoknot if two UA bps in stem 1 are present and L2 consists of only three bases instead of six; as discussed below, data exist to support that three base pairs still allow minus-strand synthesis. From in vitro studies it was previously determined that at least 11–12 A's are required for minus-strand synthesis of SINV RNA, but that 10 or fewer A's yield only 3% of minus-strand RNA (Hardy and Rice 2005). This discrepancy can have multiple causes. The in vitro assays may lack a factor that stabilizes the RNA pseudoknot and/or its inter-

action with the polymerase, and in vitro assays may also be more prone to nonnative alternative structures that compete with the pseudoknot structure. In vivo nucleotides can be added by the viral polymerase that eventually leads to a better template for minus-strand synthesis (Raju et al. 1999). These are probably added by the nsP4 subunit or a truncated form of nsP4 of the viral polymerase as shown previously (Tomar et al. 2006; Thal et al. 2007). Addition of A's in the present in vivo study is probably restricted to a few A's since
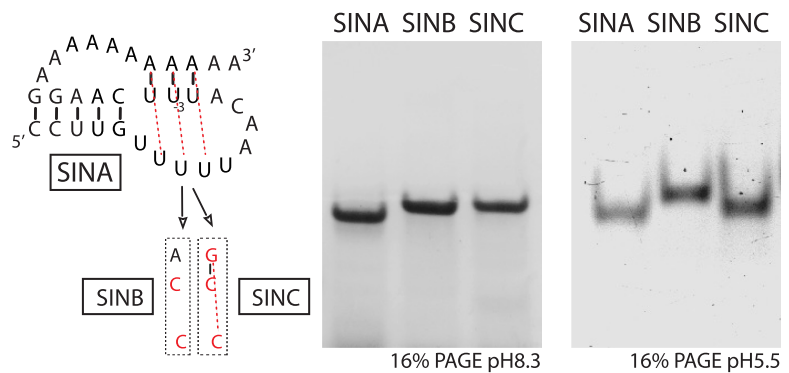
FIGURE 7. Native gel-electrophoresis at pH 8.3 and 5.5 of SINV pseudoknot RNAs with wildtype (SINA) or mutant $U_{-3}A_{+12}U_{-11}$ base triples (SINB, SINC). RNAs were visualized by Stains-All (*left* gel) or Ethidium bromide (*right* gel).
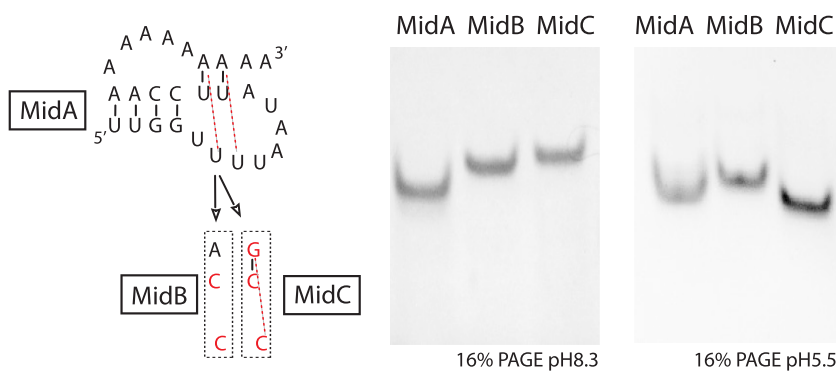
FIGURE 8. Native gel-electrophoresis at pH 8.3 and 5.5 of MIDV pseudoknot RNAs with wild-type (MidA) or mutant $U_{-3}A_{+12}U_{-11}$ base triples (MidB, MidC). RNAs were visualized by Stains-All (*upper* gel) or Ethidium bromide (*lower* gel).

constructs SinA4 and SinA0 showed very poor if no replication, whereas SinA8 may have reached the minimal 11–12 A's to show replication.

Reinterpretation of the mutations tested by Hardy and Rice (2005) with the pseudoknot model in mind leads to the following observations: mutations upstream of S1 or in the 5′ distal part of S1 do not have a large effect on replication (56%–110%, Fig. 9). With the exception of $A_{-20}A_{-19}$-to-UU mutant, these mutations reduce the length of S1 to 3 bp but do not disrupt it. The $G_{-14}A$ mutation shows 68% activity; even though the same mutation (SinZ) here showed only 22% activity, it still suggests that an AC mismatch near the junction with S2 is not very detrimental. Removal of G_{-14} would lead to C_{-1} bulging out, a situation similar to insertion of a C next to C_{-1}, both replicating at 62%. The presence of a base at the junction between two coaxially stacked stems of a pseudoknot is not uncommon (Batenburg van et al. 2000). Insertion of other nucleotides than C is more detrimental: insA (13%) and insG (18%) could base-pair with U_{-13}, thereby disrupting its Hoogsteen bp with A_{+10}, as also shown here to affect replication. insU (15%) would create a longer S2 which in the present study was shown to replicate at 77%. Changes in C_{-1} are more detrimental (G:2.2%, U:8.1%); apart from changing the stability of S1, they potentially trigger the for-

mation of alternative hairpins like A_{-25}-ACAAaauuUUGUU$_{-12}$ or U_{-15}GUUuuuAACA$_{-5}$ (stems indicated in capitals) that may compete with the pseudoknot structure.

Although deletion of C_{-1} was previously shown to be lethal for SINV replication in vivo (Kuhn et al. 1990) and in vitro (Hardy and Rice 2005), George and Raju (2000) found that the replicating virus could be obtained after deleting C_{-1}. The sequence of these replicating mutants showed insertions of six U residues directly upstream of the poly(A) tail. Furthermore, Hardy and Rice (2005) showed that template activity of the C_{-1} deletion mutant could be gradually restored from 10%–19% by inserting one to five U residues. It should be noted that these additional U's can base-pair with A's from the poly(A) tail thereby extending the length of stem S2; this may benefit the stability of the entire pseudoknot, compensating for the absence of the $G_{-14}C_{-1}$ pair.

Deletion of U_{-1} and U_{-2} (1.2%, Fig. 9, left) disrupts S2 and is therefore hardly viable. Introducing AA mismatches in S2 is more detrimental than AC mismatches (Fig. 9, middle), likely because the latter ones are less destabilizing than AA mismatches. In this study, AC mismatches in S2 retained 30%–40% activity (Fig. 4, SinJ and SinK1). Changes in the unpaired $U_{-10}AACA_{-6}$ sequence were mostly (close to) lethal (Fig. 9, middle). This is a strongly conserved motif in all alphaviruses, except for the C which is not conserved and can be replaced by other nucleotides without major effects. These results were also confirmed in this study although the "lethal" $A_{-8}C$ mutant still retained ~9% activity (Supplemental Fig. S1).

Hardy and Rice (2005) also measured the effect of inserting a row of three C's at different locations in the poly(A) tail (Fig. 9, right). Insertions near C_{-1} abolished minus-strand synthesis, likely due to distorting the stability of the pseudoknot and the orientation of stems with respect to each other.
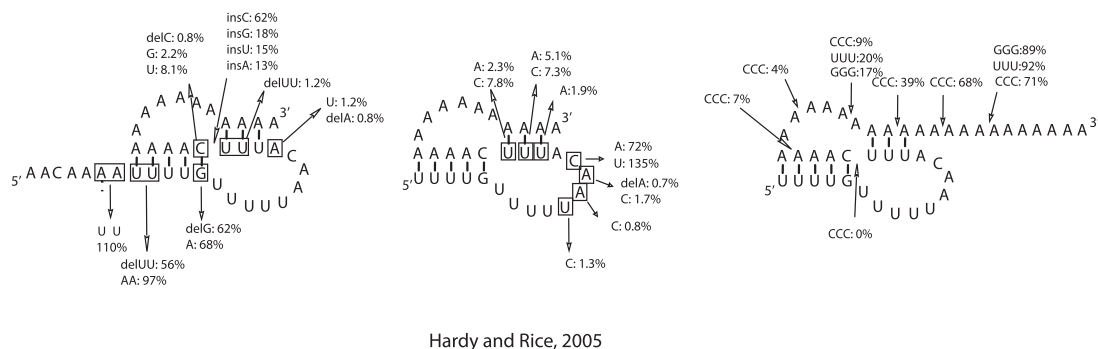
Hardy and Rice, 2005

FIGURE 9. Data from in vitro (−) RNA synthesis of Hardy and Rice (2005) in relation to the pseudoknot structure.

Insertion of CCC between A_{+3} and A_{+4} (7%), though still preserving four out of five bp in S1, changes the composition of L2 substantially, putatively disrupting A-minor interactions with S1. A-minor interactions are well-known stabilizers of pseudoknots, including the telomerase pseudoknot (Theimer et al. 2005), and also of RNA triplexes involving the poly(A) tail (Torabi et al. 2021). Likewise, insertion between A_{+6} and A_{+7} (4%) and A_{+9} and A_{+10} (9%) could affect the A-minor interactions with S1 or disrupt base pairs in S2. Insertions downstream from A_{+15} or A_{+18} had minor effects on minus-strand synthesis, most likely because they do not interfere with the pseudoknot structure.

Altogether, the proposed pseudoknot structure seems to be in agreement with the mutational analysis of the CSE by Hardy and Rice (2005).

Can the pseudoknot model for the 3-CSE explain "Raju's revertants" that were obtained after transfection of severely debilitated mutants of the CSE? (Raju et al. 1999; George and Raju 2000; James et al. 2007). Many of these mutants acquired alternating blocks of U's and A's that were added to the 3′-end of the mutated CSEs by a cellular or the viral polymerase. Careful inspection of these sequences showed that most of them can form a pseudoknot immediately preceding the poly(A) tail that resembles the wt SINV pseudoknot in many aspects, including the conserved UAANA motif and ≥2 UAU triples (Supplemental Fig. S2). A few of these alternative pseudoknots were tested in the SINV replicon. Some of these were quite successful in replication, that is, AA34 and AA35, corresponding to revertants 15.3 and S3–4 replicated at 30%–40% of wt level (Supplemental Fig. S3). Replication of five other pseudoknots, however, was poor, with levels not exceeding 3% (Supplemental Fig. S3). The fact that not all revertant sequences tested here replicated efficiently may be due to missing sequence elements that contributed to the survival of Raju's revertants, which carried up to 100 additional nucleotides. In the present assays, only the sequence that could be folded into a pseudoknot was incorporated into the replicon. Nevertheless, the viability of several of these mutants and revertants which adopt very weak pseudoknot structures (Supplemental Fig. S2) suggests that the pseudoknot or the CSE is not essential for replication. However, the pseudoknot does contribute to viral fitness as wt viruses rapidly outcompeted these mutants and revertants during a coinfection (James et al. 2007).

A similar pseudoknot involving the poly(A) tail is present at the 3′-end of Bamboo Mosaic Virus (BaMV) RNA (Tsai et al. 1999). BaMV is a plant virus of the *Alphaflexiviridae* family which is part of the Alphavirus superfamily and is closely related to alphaviruses based on conserved motifs in their RdRps. For BaMV, the requirement of the pseudoknot by itself for replication has not been tested, because this would require mutation of the poly(A) sequence as well. Recent data suggest that the BaMV pseudoknot is also stabilized by UAU triples and that a similar pseudoknot is present in the majority of potexviruses and viruses of the *Betaflexiviridae* (Olsthoorn et al. 2022).

Interestingly, BaMV minus-strand synthesis has been found to start from several sites within the poly(A) tail, with the majority starting at position A_{+7} in L2 (Cheng et al. 2002). This differs from findings with SINV by Hardy (2006), who found that minus-strand synthesis occurs opposite of C_{-1} using in vitro assays. On the other hand, (−) RNA isolated in vivo was found to contain at least 60 U residues at the 5′ end, suggesting that replication initiates within the poly(A) tail (Sawicki and Gomatos 1976; Frey and Strauss 1978). Also, many of the revertants found by Raju and coworkers (Raju et al. 1999; George and Raju 2000) actually stably maintain A and U insertions downstream from C_{-1} in their genome for many passages. The observation that all-A/U pseudoknots in this study (AA34 and AA35) replicated efficiently also suggests that minus-strand synthesis in vivo starts at a different position than in vitro, possibly owing to different reaction conditions.

The SINV pseudoknot is stabilized by UAU base triples and in this respect shows resemblance to other RNAs like KSHV and telomerase pseudoknots. By mutational analysis it was demonstrated that the SINV triples are not in the KSHV-like register but adopt the telomerase-like structure, leaving U_{-13} to form a Hoogsteen Watson–Crick base pair with an A in the poly(A) tail by analogy with the human telomerase PK (Fig. 10). Mutation of this potential Hoogsteen bp in SINV led to a substantial decrease in replication, similar to the effects on the human telomerase PK (Theimer et al. 2005). Replacing U_{-13} by a G was less detrimental than the U_{-13} to C change, probably because G can also form a Hoogsteen pair with A_{+10}. The structural similarity with the telomerase PK also suggests that A-minor interactions of the A_{+8} and A_{+9} have a stabilizing role in SINV PK (Fig. 10). Their contribution could not be tested in this work due to the fact that the loop size of L2 is quite flexible, so that changing these two particular A's can easily be compensated by neighboring A's in the poly(A) tail. Future experiments using, for example, the SinP mutant as a scaffold in which the loop size of L2 is fixed by the CGC triple would allow for such studies.

In terms of stability, the SINV PK would be expected to be much weaker than the human telomerase PK even though both structures are active at 37°C. For native gel electrophoresis, it was necessary to replace some of the AU pairs in S1 with GC pairs in SINA RNA to obtain well-resolved bands on gel. However, the smaller MIDV pseudoknot was stable under these conditions, suggesting that a stem S2 of just 2 AU bps is feasible when stabilized by base triples. Interestingly, some of the telomerase PKs that are present in *Tetrahymena* species are AU-rich as well (Fig. 10). The *T. thermophila* PK reportedly is not very stable, being in an equilibrium with an alternating hairpin structure (Cash and Feigon 2017). It is likely that the alphavirus PKs

FIGURE 10. Comparison of alphavirus and telomerase pseudoknots. (*A*) Similarities between SINV and human and tetrahymena telomerase pseudoknots. Green dotted lines indicate A-minor interactions, red dotted lines indicate Hoogsteen base pairs, and black dashes Watson–Crick base pairs. The interactions in *T. pigmentosa* are drawn by analogy to the *T. thermophila* pseudoknot (Cash and Feigon 2017). (*B*) Detailed models of the MIDV and SINV pseudoknots are drawn to resemble the human telomerase pseudoknot (Theimer et al. 2005).

are also in equilibrium with a hairpin which may have a different function in the lifecycle of the virus, for instance favoring translation. Pseudoknots at the 3′-end of viral RNAs may fulfill such a role with or without the help of viral or host proteins (Olsthoorn et al. 1999; Dreher 2009). These alternating structures in viral RNAs could be promising targets for small molecule drugs that interfere with viral replication by shifting the equilibrium toward one or the other side. Recently, using high-throughput screening approaches, small molecule ligands have been identified that either bind the triple helix of MALAT1 noncoding RNA or its hairpin conformation (Donlic et al. 2018; Abulwerdi et al. 2019). Similar HTS approaches directed at the alphavirus pseudoknot could eventually lead to an effective antiviral against encephalitis and Chikungunya.

MATERIALS AND METHODS

Constructs

Templates for full-length SINV RNA were obtained by PCR on the Sinrep5 plasmid (kindly provided by Dr. P. Bredenbeek, Leiden University Medical Center) using forward primer SP6SIN and several reverse primers (Supplemental Table 1). PCR conditions were: 95°C for 3 min, then 30 cycles at 94°C for 1 min, 55°C for 45 sec, 68°C for 5 min, followed by 5 min at 72°C. PCR reactions were carried out in a 50 µL volume containing 400 nM of each oligo, 200 µM dNTPs and two units of DreamTaq polymerase (Thermo Fisher) on a BioRad cycler. PCR products were purified by NaAc/EtOH precipitation, washed with 70% EtOH, and after drying dissolved in Milli-Q water.

Sinrep-Nluc was constructed by digestion of Sinrep5 plasmid with Xba and StuI and insertion of an NheI-XbaI (blunted by T4 DNA polymerase) fragment containing the Nluc gene of pNL1.1

(Promega, Benelux). The RLuc-SIN-3UTR plasmid was obtained by insertion of a PCR fragment covering the SINV 3′-UTR into a *Renilla* luciferase reporter plasmid previously described (Girard et al. 2011). The XbaI-XhoI fragment of this vector was replaced with the XbaI-XhoI digested SIN-UTR PCR fragment. Templates for transcription were obtained by PCR using forward primer SP6FLU and reverse primers (Supplemental Table S1).

Transcription

RiboMAX Large Scale RNA Production Systems (Promega, Benelux) and HiScribe SP6 RNA Synthesis Kits (New England BioLabs) were used for transcription. Reactions were carried out in 5 or 10 µL volumes containing 100–200 ng of PCR template DNA, ATP, CTP, UTP (10 mM each), 2 mM 3′-O-Me-m^{7}G(5′)ppp (5′)G cap structure analog (NEB S1411S), 0.5 mM GTP, 0.5–1 unit of RNase-inhibitor (RNasin, Promega), and 0.5–1 µL of enzyme mix. Incubation was done at 37°C for 2.5 h. Quality and quantity of transcripts were checked on agarose gels.

Transfection

A total of 100 ng of transcript (as judged by gel electrophoresis) was mixed with Dulbecco's Modified Eagle's Medium (DMEM) and 0.5 µL of MessengerMax lipofectamine (Invitrogen) premixed with DMEM, and after 20 min incubation at RT added to a well of a 48-well plate containing BHK21J cells at ~70% confluency. Cells were grown at 37°C in 5% CO_2 on growth medium consisting of DMEM supplemented with 10% GlutaMAX (Thermo Fisher), ampicillin, streptomycin, and fetal calf serum, and analyzed 20–24 h after transfection. Fluorescent microscopy was performed on an EVOS FL Auto Imaging System (Fisher Scientific). Luciferase activity was measured after lysis of cells using Passive Lysis Buffer (Promega) and transferring the contents to a 96-well plate to which the appropriate substrate was added and assayed using a GloMax Multi System (Promega).

Native PAGE

RNA oligonucleotides were purchased from Merck (Sigma-Aldrich) at 0.05 nmole scale/desalted. A total of 100–200 pmoles of each RNA was loaded onto polyacrylamide gels containing 12% or 16% acrylamide:bisacrylamide (19:1), Tris (40 mM), acetate (20 mM), EDTA (1 mM) pH 8.3, to which 2.5 mM MgAc$_2$ was added. Gels were run in TAEM buffer at ~85 V and 12 mA for ~4 h in a cold room. For acidic PAGE, the pH was adjusted by addition of acetic acid to all buffers involved. RNA was visualized by EtBr or Stains-All staining.

SUPPLEMENTAL MATERIAL

Supplemental material is available for this article.

ACKNOWLEDGMENTS

REFERENCES

Abulwerdi FA, Xu W, Ageeli AA, Yonkunas MJ, Arun G, Nam H, Schneekloth JS, Dayie TK, Spector D, Baird N, et al. 2019. Selective small-molecule targeting of a triple helix encoded by the long noncoding RNA, MALAT1. *ACS Chem Biol* **14:** 223–235. doi:10.1021/acschembio.8b00807

Ahlquist P. 1992. Bromovirus RNA replication and transcription. *Curr Opin Genet Dev* **2:** 71–76. doi:10.1016/s0959-437x(05)80325-9

Akiyama BM, Laurence HM, Massey AR, Costantino DA, Xie X, Yang Y, Shi PY, Nix JC, Beckham JD, Kieft JS. 2016. Zika virus produces noncoding RNAs using a multi-pseudoknot structure that confounds a cellular exonuclease. *Science* **354:** 1148–1152. doi:10.1126/science.aah3963

Batenburg van FH, Gultyaev AP, Pleij CWA, Ng J, Oliehoek J. 2000. PseudoBase: a database with RNA pseudoknots. *Nucleic Acids Res* **28:** 201–204. doi:10.1093/nar/28.1.201

Bhatt PR, Scaiola A, Loughran G, Leibundgut M, Kratzel A, Meurs R, Dreos R, O'Connor KM, McMillan A, Bode JW, et al. 2021. Structural basis of ribosomal frameshifting during translation of the SARS-CoV-2 RNA genome. *Science* **372:** 1306–1313. doi:10.1126/science.abf3546

Bredenbeek PJ, Frolov I, Rice CM, Schlesinger S. 1993. Sindbis virus expression vectors: packaging of RNA replicons by using defective helper RNAs. *J Virol* **67:** 6439–6446. doi:10.1128/JVI.67.11.6439-6446.1993

Brierley I, Digard P, Inglis SC. 1989. Characterization of an efficient coronavirus ribosomal frameshifting signal: requirement for an RNA pseudoknot. *Cell* **57:** 537–547. doi:10.1016/0092-8674(89)90124-4

Brown JA, Valenstein ML, Yario TA, Tycowski KT, Steitz JA. 2012. Formation of triple-helical structures by the 3′-end sequences of MALAT1 and MENβ noncoding RNAs. *Proc Natl Acad Sci* **109:** 19202–19207. doi:10.1073/pnas.1217338109

Carey J, Cameron V, de Haseth PL, Uhlenbeck OC. 1983. Sequence-specific interaction of R17 coat protein with its ribonucleic acid binding site. *Biochemistry* **22:** 2601–2610. doi:10.1021/bi00280a002

Cash DD, Feigon J. 2017. Structure and folding of the *Tetrahymena* telomerase RNA pseudoknot. *Nucleic Acids Res* **45:** 482–495. doi:10.1093/nar/gkw1153

Charrel RN, de Lamballerie X, Raoult D. 2007. Chikungunya outbreaks —the globalization of vectorborne diseases. *N Engl J Med* **356:** 769–771. doi:10.1056/NEJMp078013

Cheng JH, Peng CW, Hsu YH, Tsai CH. 2002. The synthesis of minus-strand RNA of bamboo mosaic potexvirus initiates from multiple sites within the poly(A) tail. *J Virol* **76:** 6114–6120. doi:10.1128/jvi.76.12.6114-6120.2002

Devi G, Zhou Y, Zhong Z, Toh DK, Chen G. 2015. RNA triplexes: from structural principles to biological and biotech applications. *Wiley Interdiscip Rev RNA* **6:** 111–128. doi:10.1002/wrna.1261

Dilweg IW, Gultyaev AP, Olsthoorn RCL. 2019. Structural features of an Xrn1-resistant plant virus RNA. *RNA Biol* **16:** 838–845. doi:10.1080/15476286.2019.1592070

Ding P, Kharytonchyk S, Waller A, Mbaekwe U, Basappa S, Kuo N, Frank HM, Quasney C, Kidane A, Swanson C, et al. 2020. Identification of the initial nucleocapsid recognition element in the HIV-1 RNA packaging signal. *Proc Natl Acad Sci* **117:** 17737–17746. doi:10.1073/pnas.2008519117

Donlic A, Morgan BS, Xu JL, Liu A, Roble C Jr, Hargrove AE. 2018. Discovery of small molecule ligands for MALAT1 by tuning an RNA-binding scaffold. *Angew Chem Int Ed Engl* **57:** 13242–13247. doi:10.1002/anie.201808823

Dreher TW. 2009. Role of tRNA-like structures in controlling plant virus replication. *Virus Res* **139:** 217–229. doi:10.1016/j.virusres.2008.06.010

Flobinus A, Hleibieh K, Klein E, Ratti C, Bouzoubaa S, Gilmer D. 2016. A viral noncoding RNA complements a weakened viral RNA silencing suppressor and promotes efficient systemic host infection. *Viruses* **8:** 272. doi:10.3390/v8100272

Frey TK, Strauss JH. 1978. Replication of Sindbis virus: VI. Poly(A) and poly(U) in virus-specific RNA species. *Virology* **86:** 494–506. doi:10.1016/0042-6822(78)90088-0

Frolov I, Hardy R, Rice CM. 2001. *Cis*-acting RNA elements at the 5′ end of Sindbis virus genome RNA regulate minus- and plus-strand RNA synthesis. *RNA* **7:** 1638–1651. doi:10.1017/s1355838201010101x

Frolova E, Frolov I, Schlesinger S. 1997. Packaging signals in alphaviruses. *J Virol* **71:** 248–258. doi:10.1128/JVI.71.1.248-258.1997

George J, Raju R. 2000. Alphavirus RNA genome repair and evolution: molecular characterization of infectious Sindbis virus isolates lacking a known conserved motif at the 3′ end of the genome. *J Virol* **74:** 9776–9785. doi:10.1128/jvi.74.20.9776-9785.2000

Girard G, Gultyaev AP, Olsthoorn RCL. 2011. Upstream start codon in segment 4 of North American H2 avian influenza A viruses. *Infect Genet Evol* **11:** 489–495. doi:10.1016/j.meegid.2010.12.014

Hardy RW. 2006. The role of the 3′ terminus of the Sindbis virus genome in minus-strand initiation site selection. *Virology* **345:** 520–531. doi:10.1016/j.virol.2005.10.018

Hardy RW, Rice CM. 2005. Requirements at the 3′ end of the Sindbis virus genome for efficient synthesis of minus-strand RNA. *J Virol* **79:** 4630–4639. doi:10.1128/JVI.79.8.4630-4639.2005

Hyde JL, Chen R, Trobaugh DW, Diamond MS, Weaver SC, Klimstra WB, Wilusz J. 2015. The 5′ and 3′ ends of alphavirus RNAs—non-coding is not non-functional. *Virus Res* **206:** 99–107. doi:10.1016/j.virusres.2015.01.016

Jaafar ZA, Kieft JS. 2019. Viral RNA structure-based strategies to manipulate translation. *Nat Rev Microbiol* **17:** 110–123. doi:10.1038/s41579-018-0117-x

James FD, Hietala KA, Eldar D, Guess TE, Cone C, Mundell NA, Barnett JV, Raju R. 2007. Efficient replication, and evolution of

Sindbis virus genomes with non-canonical 3′A/U-rich elements (NC3ARE) in neonatal mice. *Virus Genes* **35:** 651–662. doi:10.1007/s11262-007-0130-z

Kendall C, Khalid H, Müller M, Banda DH, Kohl A, Merits A, Stonehouse NJ, Tuplin A. 2019. Structural and phenotypic analysis of Chikungunya virus RNA replication elements. *Nucleic Acids Res* **47:** 9296–9312. doi:10.1093/nar/gkz640

Kim DY, Firth AE, Atasheva S, Frolova EI, Frolov I. 2011. Conservation of a packaging signal and the viral genome RNA packaging mechanism in alphavirus evolution. *J Virol* **85:** 8022–8036. doi:10.1128/JVI.00644-11

Kolk MH, van der Graaf M, Wijmenga SS, Pleij CW, Heus HA, Hilbers CW. 1998. NMR structure of a classical pseudoknot: interplay of single- and double-stranded RNA. *Science* **280:** 434–438.

Kuhn RJ, Hong Z, Strauss JH. 1990. Mutagenesis of the 3′ nontranslated region of Sindbis virus RNA. *J Virol* **64:** 1465–1476. doi:10.1128/JVI.64.4.1465-1476.1990

Levi LI, Vignuzzi M. 2019. Arthritogenic alphaviruses: a worldwide emerging threat? *Microorganisms* **7:** E133. doi:10.3390/microorganisms7050133

Levis R, Weiss BG, Tsiang M, Huang H, Schlesinger S. 1986. Deletion mapping of Sindbis virus DI RNAs derived from cDNAs defines the sequences essential for replication and packaging. *Cell* **44:** 137–145. doi:10.1016/0092-8674(86)90492-7

Levis R, Schlesinger S, Huang HV. 1990. Promoter for Sindbis virus RNA-dependent subgenomic RNA transcription. *J Virol* **64:** 1726–1733. doi:10.1128/JVI.64.4.1726-1733.1990

Liu Y, Wimmer E, Paul AV. 2009. *Cis*-acting RNA elements in human and animal plus-strand RNA viruses. *Biochim Biophys Acta* **1789:** 495–517. doi:10.1016/j.bbagrm.2009.09.007

Liu Y, Zhang Y, Wang M, Cheng A, Yang Q, Wu Y, Jia R, Liu M, Zhu D, Chen S, et al. 2020. Structures and functions of the 3′ untranslated regions of positive-sense single-stranded RNA viruses infecting humans and animals. *Front Cell Infect Microbiol* **10:** 453. doi:10.3389/fcimb.2020.00453

Masters PS. 2019. Coronavirus genomic RNA packaging. *Virology* **537:** 198–207. doi:10.1016/j.virol.2019.08.031

Miras M, Miller WA, Truniger V, Aranda MA. 2017. Non-canonical translation in plant RNA viruses. *Front Plant Sci* **8:** 494. doi:10.3389/fpls.2017.00494

Mitton-Fry RM, DeGregorio SJ, Wang J, Steitz TA, Steitz JA. 2010. Poly(A) tail recognition by a viral RNA element through assembly of a triple helix. *Science* **330:** 1244–1247. doi:10.1126/science.1195858

Morrison TE. 2014. Reemergence of chikungunya virus. *J Virol* **88:** 11644–11647. doi:10.1128/JVI.01432-14

Niesters HG, Strauss JH. 1990. Mutagenesis of the conserved 51-nucleotide region of Sindbis virus. *J Virol* **64:** 1639–1647. doi:10.1128/JVI.64.4.1639-1647.1990

Olsthoorn RC, Mertens S, Brederode FT, Bol JF. 1999. A conformational switch at the 3′ end of a plant virus RNA regulates viral replication. *EMBO J* **18:** 4856–4864. doi:10.1093/emboj/18.17.4856

Olsthoorn RCL, Owen CA, Livieratos IC. 2022. Role of an RNA pseudoknot involving the polyA tail in replication of *Pepino mosaic potexvirus* and related plant viruses. *Sci Rep* **12:** 11532. doi:10.1038/s41598-022-15598-5

Pfeffer M, Kinney RM, Kaaden OR. 1998. The alphavirus 3′-nontranslated region: size heterogeneity and arrangement of repeated sequence elements. *Virology* **240:** 100–108. doi:10.1006/viro.1997.8907

Pflug A, Guilligay D, Reich S, Cusack S. 2014. Structure of influenza A polymerase bound to the viral RNA promoter. *Nature* **516:** 355–360. doi:10.1038/nature14008

Pijlman GP, Funk A, Kondratieva N, Leung J, Torres S, van der Aa L, Liu WJ, Palmenberg AC, Shi PY, Hall RA, et al. 2008. A highly structured, nuclease-resistant, noncoding RNA produced by flaviviruses is required for pathogenicity. *Cell Host Microbe* **4:** 579–591. doi:10.1016/j.chom.2008.10.007

Pilipenko EV, Maslova SV, Sinyakov AN, Agol VI. 1992. Towards identification of *cis*-acting elements involved in the replication of enterovirus and rhinovirus RNAs: a proposal for the existence of tRNA-like terminal structures. *Nucleic Acids Res* **20:** 1739–1745. doi:10.1093/nar/20.7.1739

Pleij CW, Rietveld K, Bosch L. 1985. A new principle of RNA folding based on pseudoknotting. *Nucleic Acids Res* **13:** 1717–1731. doi:10.1093/nar/13.5.1717

Pogany J, Fabian MR, White KA, Nagy PD. 2003. A replication silencer element in a plus-strand RNA virus. *EMBO J* **22:** 5602–5611. doi:10.1093/emboj/cdg523

Raju R, Hajjou M, Hill KR, Botta V, Botta S. 1999. *In vivo* addition of poly(A) tail and AU-rich sequences to the 3′ terminus of the Sindbis virus RNA genome: a novel 3′-end repair pathway. *J Virol* **73:** 2410–2409. doi:0.1128/JVI.73.3.2410-2419.1999

Ramachandran V, Malaisamy M, Ponnaiah M, Kaliaperuaml K, Vadivoo S, Gupte MD. 2012. Impact of Chikungunya on health related quality of life Chennai, South India. *PLoS ONE* **7:** e51519. doi:10.1371/journal.pone.0051519

Rietveld K, Pleij CW, Bosch L. 1983. Three-dimensional models of the tRNA-like 3′ termini of some plant viral RNAs. *EMBO J* **2:** 1079–1085. doi:10.1002/j.1460-2075.1983.tb01549.x

Sawicki DL, Gomatos PJ. 1976. Replication of Semliki Forest virus: polyadenylate in plus-strand and polyuridylate in minus-strand RNA. *J Virol* **20:** 446–464. doi:10.1128/JVI.20.2.446-464.1976

Thal MA, Wasik BR, Posto J, Hardy RW. 2007. Template requirements for recognition and copying by Sindbis virus RNA-dependent RNA polymerase. *Virology* **358:** 221–232. doi:10.1016/j.virol.2006.08.022

Theimer CA, Blois CA, Feigon J. 2005. Structure of the human telomerase RNA pseudoknot reveals conserved tertiary interactions essential for function. *Mol Cell* **17:** 671–682. doi:10.1016/j.molcel.2005.01.017

Tomar S, Hardy RW, Smith JL, Kuhn RJ. 2006. Catalytic core of alphavirus nonstructural protein nsP4 possesses terminal adenylyltransferase activity. *J Virol* **80:** 9962–9969. doi:10.1128/JVI.01067-06

Torabi SF, Vaidya AT, Tycowski KT, DeGregorio SJ, Wang J, Shu MD, Steitz TA, Steitz JA. 2021. RNA stabilization by a poly(A) tail 3′-end binding pocket and other modes of poly(A)-RNA interaction. *Science* **371:** eabe6523. doi:10.1126/science.abe6523

Tsai CH, Cheng CP, Peng CW, Lin BY, Lin NS, Hsu YH. 1999. Sufficient length of a poly(A) tail for the formation of a potential pseudoknot is required for efficient replication of bamboo mosaic potexvirus RNA. *J Virol* **73:** 2703–2709. doi:10.1128/JVI.73.4.2703-2709.1999

Turner DR, Joyce LE, Butler PJ. 1988. The tobacco mosaic virus assembly origin RNA. Functional characteristics defined by directed mutagenesis. *J Mol Biol* **203:** 531–547. doi:10.1016/0022-2836(88)90190-8

You S, Rice CM. 2008. 3′ RNA elements in hepatitis C virus replication: kissing partners and long poly(U). *J Virol* **82:** 184–195. doi:10.1128/JVI.01796-07

Zuker M. 2003. Mfold web server for nucleic acid folding and hybridization prediction. *Nucleic Acids Res* **31:** 3406–3415. doi:10.1093/nar/gkg595